NREL
NATIONAL RENEWABLE ENERGY LABORATORY

Assessing the Importance of Nonlinearities in the Development of a Substructure Model for the Wind Turbine CAE Tool FAST

Preprint

R. Damiani, J. Jonkman, A. Robertson, and H. Song

To be presented at the 32nd International Conference on Ocean, Offshore and Arctic Engineering
Nantes, France
June 9-14, 2013

NREL is a national laboratory of the U.S. Department of Energy, Office of Energy Efficiency & Renewable Energy, operated by the Alliance for Sustainable Energy, LLC.

Conference Paper
NREL/CP-5000-57850
March 2013

Contract No. DE-AC36-08GO28308

Available electronically at http://www.osti.gov/bridge

Available for a processing fee to U.S. Department of Energy
and its contractors, in paper, from:

U.S. Department of Energy
Office of Scientific and Technical Information
P.O. Box 62
Oak Ridge, TN 37831-0062
phone: 865.576.8401
fax: 865.576.5728
email: mailto:reports@adonis.osti.gov

Available for sale to the public, in paper, from:

U.S. Department of Commerce
National Technical Information Service
5285 Port Royal Road
Springfield, VA 22161
phone: 800.553.6847
fax: 703.605.6900
email: orders@ntis.fedworld.gov
online ordering: http://www.ntis.gov/help/ordermethods.aspx

Cover Photos: (left to right) PIX 16416, PIX 17423, PIX 16560, PIX 17613, PIX 17436, PIX 17721

Printed on paper containing at least 50% wastepaper, including 10% post consumer waste.

ASSESSING THE IMPORTANCE OF NONLINEARITIES IN THE DEVELOPMENT OF A SUBSTRUCTURE MODEL FOR THE WIND TURBINE CAE TOOL FAST

Rick R. Damiani
National Renewable Energy Laboratory
Golden, CO, USA

Huimin Song
National Renewable Energy Laboratory
Golden, CO, USA

Amy N. Robertson
National Renewable Energy Laboratory
Golden, CO, USA

Jason M. Jonkman
National Renewable Energy Laboratory
Golden, CO, USA

ABSTRACT

The design and analysis of wind turbines are performed using aero-servo-elastic tools that account for the nonlinear coupling between aerodynamics, controls, and structural response. The NREL-developed computer-aided engineering (CAE) tool FAST also resolves the hydrodynamics of fixed-bottom structures and floating platforms for offshore wind applications.

Primarily due to the required modal characteristics, monopiles become progressively less economical and more difficult (or impossible) to fabricate for multimegawatt turbines and water depths of more than 25–30 m. Derived from the oil and gas industry experience, light and stiff space-frame alternatives have been proposed to alleviate this problem. Lattice structures (e.g., jackets) are more complex to analyze and design than cantilevered monopiles, especially in terms of the structural dynamics of the coupled turbine-support structure system.

This paper outlines the implementation of a structural-dynamics module (SubDyn) for offshore wind turbines with space-frame substructures into the current FAST framework, and in particular focuses on the initial assessment of the importance of structural nonlinearities. Nonlinear effects include: large displacements, axial shortening due to bending, cross-sectional transverse shear effects, etc. A nonlinear computational analysis is resource-intensive, thus it is important to assess the applicability of a linear approach to maintain high-fidelity results while still allowing for fast and efficient design simulations. Space-frame structural behavior can be controlled by a number of design parameters (e.g., member cross-sectional properties, number of legs, batter angles). Additionally, nonlinearities may manifest only at certain load levels. Several finite-element analyses were carried out via commercial and open-source codes that can capture nonlinear effects in the structural behavior of turbine substructures under different load cases. Results were compared to the output of the new linear module SubDyn. The configurations considered in this study included 5-MW, 7-MW, and 10-MW platforms: OC3[1] monopile, OC3 tripod, OC4[2] jacket, and a full-lattice tower, all supporting a 5-MW turbine; also two jackets for a 7-MW and a 10-MW turbine, respectively, were investigated. These models differed in base geometry, load paths, size, supported towers, and turbine masses. Results showed that nonlinearities (quantified in terms of the maximum differences in displacement and stresses with respect to a linear calculation) amounted to about 4% (3%) at tower top (at tower base), or about 10 cm (1 cm). This means that the absolute effects of nonlinearities are mostly associated with the tower. The linear approach used by the multimember structural module introduced in this paper was therefore deemed suitable to be utilized within FAST to analyze multimember substructures for offshore wind applications.

Keywords: Offshore Turbine Support, Nonlinear Analysis, Turbine Substructure, Beam Finite Element, Multimember, Turbine Jacket

1. INTRODUCTION

Offshore wind power generation can take advantage of a large wind resource with reduced turbulence levels; generally fewer real-estate constraints than on land; and the proximity to major metropolitan load centers [1]. Yet, because of the costs associated with the balance of system (BOS, attributable to

[1] Offshore Code Comparison Collaboration
[2] Offshore Code Comparison Collaboration Continuation

higher foundation and installation costs) as well as with operation and maintenance (O&M), presently, electricity from offshore wind is considerably more expensive than its land-based counterpart.

Offshore wind costs may be reduced by providing access to the higher winds flowing over water at transitional depths (30-m to 60-m depth, and 5 nm to 50 nm from shore). Preliminary resource assessments for the United States have shown that the transitional-depth resource for Class 4 wind and above exceeds 600 GW [2].

Most of the offshore development to date has occurred in Europe, where turbines have primarily been installed in shallow waters (<30 m) and on monopiles. A few wind farms have been sited in transitional waters (e.g., Alpha Ventus, Beatrice, Bard) where either tripods, tripiles, or jackets have been employed as substructures.

Several studies [3,4] have shown that monopiles become progressively unfeasible for deeper waters and larger turbine sizes (>5 MW). The main obstacle to monopile deployment is the large size needed to guarantee modal performance (e.g. resonance avoidance), which translates into very large structural mass (varying cubically with depth) and expensive or prohibitive manufacturing and installation costs. Lattice structures can deliver needed stiffness by increasing the footprint of the substructure, while balancing manufacturability and material costs.

The analysis of a lattice structure with moment connections is more challenging than that of a monopile. To guarantee both structural integrity and dynamic characteristics suitable to the deployment of a wind turbine, accurate coupled-modeling of wind/wave inflow fields, aerodynamics, hydrodynamics, soil-structure interaction, structural dynamic response, and controls is required.

The National Renewable Energy Laboratory (NREL), sponsored by the U.S. Department of Energy, has developed a number of tools that revolve around the main aeroelastic computer-aided-engineering (CAE) tool FAST [5]. FAST is capable of aero-hydro-servo-elastic analysis of land-based and offshore wind turbines. Until recently, FAST was limited to tower/monopile and floating hull configurations. FAST, through a combined modal and multibody dynamics approach, captures many nonlinearities within its structural model for tower and blades. Considerable effort has been put into improving the overall modularity of FAST [6] through a new framework that allows enhanced flexibility and functionality development.

Within this framework, a new module (SubDyn) was developed to address the structural dynamic response of multimember substructures (e.g., jackets and tripods). Additionally, HydroDyn, a module for hydrodynamic loading was upgraded to model the hydrodynamic loading on these kinds of substructures [7]. SubDyn is based on a linear finite-element model and linear dynamic system reduction, and its fundamental theory and mathematical approach are described in a companion paper [8]. This paper discusses some aspects of the SubDyn development, particularly the assessment of potential structural nonlinearities of offshore wind support structures through the analysis of a few example configurations. This assessment helped decide whether a linear or nonlinear approach would be used in SubDyn.

Nonlinear effects include large displacements, axial shortening due to bending, cross-sectional transverse shear effects, etc. A nonlinear computational analysis of the substructure is highly resource intensive and may not be affordable in preliminary design phases. The certification-driven design process is, in fact, iterative and extensive, as it must consider a vast set of environmental conditions and operational scenarios. CAE tools such as FAST are required to run swiftly on typical workstations. It is therefore essential to verify the applicability of the linear approach in SubDyn to maintain high fidelity results while allowing for fast and efficient design simulations.

Six case studies were included in this paper: a monopile, a tripod, three jacket configurations, and an all-lattice tower. The various geometries are characterized by different tower-top masses, different loading levels, and different overall lengths. The analyses were carried out in ANSYS (*ANSYS® Structural, Release 14.0*), GEBT [9], and SubDyn.

In this paper, Section 2 provides an overview of the recently developed SubDyn module and a brief description of the method employed by the other codes used to assess nonlinearities of the offshore substructures. Sections 3 and 4 present two reference examples for a monopile and a tripod configuration. Sections 5 through 7 examine nonlinearity effects for jacket/tower configurations for 5-MW, 7-MW, and 10-MW turbines. Section 8 concludes the case studies with an all-lattice support structure for a 5-MW turbine. Conclusions and current and anticipated future research are summarized in Section 9.

2. OVERVIEW OF THE SUBDYN MODULE AND STRATEGY OF THIS STUDY

SubDyn has been developed within the new FAST modularization framework [6], which allows for ease of maintainability, upgradability, and interfacing with other functionalities. The module strives to maintain a high degree of flexibility and physical resolution while allowing for the rapid aero-hydro-servo-elastic simulations that are needed in the design process of an offshore wind turbine. This paper only provides a brief introduction of the SubDyn module; more details can be found in [8].

The module is based on a linear finite-element method (FEM) and a Craig-Bampton dynamic system reduction.

The FEM is built upon a linear beam theory and can make use of multiple element formulations. The user can select Euler-Bernoulli beam elements, as well as Timoshenko beam elements, either tapered or of constant cross-section. The order of the element representation (shape functions) is either linear or quadratic, and there is ample flexibility in the treatment of cross-sectional stiffness and geometric characteristics.

Given the typical number of joints in an offshore space-frame structure (e.g., jacket), the number of FEM nodal degrees of freedom (DOFs) can grow rapidly into the hundreds. If

more resolution is requested via multiple elements in each member, the number of DOFs can rise into the thousands. In contrast, in the typical FAST combined modal and multibody formulation, the turbine system is represented by about 20 DOFs. For this reason, a reduced finite-element model is sought via the Craig-Bampton method [10]. With this method, the discretized structure is transformed from a set of physical coordinates to a hybrid set of physical coordinates at the boundary (interface), and modal (generalized) coordinates in the interior. By truncating the set of modal solutions to a smaller subset, the number of DOFs is easily reduced to just a few (<10). The reason this is practical is that higher frequency modes have little contribution to the dynamic response to low-frequency forcing. Similar to land-based turbines, the response of offshore wind turbines can be characterized by the superposition of relatively low frequency modes, because the wave excitation resides at the low end of the dynamic spectrum (<0.3 Hz). The Craig-Bampton reduction, however, can only be applied to a linear system.

Loads are transferred to the substructure via the HydroDyn [7] hydrodynamic module, and through the interface nodes at the base of the tower. In this paper, SubDyn was used to model both the tower and the substructure and their connection (transition piece). Normally, this would not be the case, and the TP and tower would be treated in FAST's structural module ElastoDyn.

The substructure is generally considered clamped at the base nodes (leg feet), but other restraint layouts can be envisaged and implemented via the SubDyn input file. In the future, a soil-pile interaction module will be implemented.

The efficiency of the code is thus somewhat intrinsically maintained via the above described methodology, but the linear beam-element formulation needs to be verified, for nonlinearities may be important in the overall structural response. This study was used to determine whether the linear approach was in fact suitable as a basis for SubDyn.

In the following sections, the results from the SubDyn FEM module (without Craig-Bampton reduction) are compared to analogous data output by GEBT and ANSYS for a few offshore support configurations under different loading scenarios. The intent of this comparison is to verify the applicability of SubDyn and to quantify the nonlinear effects.

GEBT—based on the geometrically exact beam theory (GEBT) of the same name—is developed based on the asymptotically reduced beam theory [11]. It makes use of a mixed variational formulation for the derivation of the equations of motion and can systematically capture all geometrical nonlinearities attainable by the Timoshenko beam model. GEBT can predict linear/nonlinear static/dynamic (both steady state and transient) behavior, as well as eigenfrequencies and mode shapes. It uses the lowest possible shape functions through a mixed formulation, and the element matrices are calculated exactly without numerical integration. The GEBT theory (not the GEBT tool of the same name) is currently being applied to the blade structural dynamics in FAST, where nonlinear effects cannot be disregarded for particularly soft and flexible layouts.

Unfortunately, the authors could not achieve accurate results with GEBT in cases where the transition piece between substructure and tower had to be simulated as a rigid connection. Therefore, those results are not shown in this study.

ANSYS is a commercial FEM package that can account for multiple nonlinearities, including geometrical effects (large deformations), material nonlinear behavior, and stress-stiffening effects. We used pipe288 and beam188 elements for straight (e.g. monopile, jacket leg and brace) and tapered (e.g. tower) members respectively, which are quadratic, two-node elements based on Timoshenko beam theory.

The tools' results were compared in terms of calculated mass, eigenfrequencies, and displacements under given turbine thrust loads assumed as applied at the centers of mass of the rotor-nacelle assemblies (RNAs). In this study, the simulations were run in an uncoupled fashion, without direct interaction with aerodynamics, hydrodynamics, and turbine control. Wind loads are normally the primary driving loads for an offshore wind turbine structure [12], and for the sake of simplicity, we ignored wave loads in this study. In most cases, to allow for a better comparison among the tools' results, weight loading was limited to concentrated forces because GEBT does not include a direct way to account for self-weight. Moreover, for simplicity, the modal analysis ignored any damping in this study.

The thrust loads were varied across ranges determined by the expected values under normal operation and extreme event conditions (lower bounds) up to values that would cause yield of the material in a limited region of the support (upper bounds). Yield strength was assumed at 345 MPa (e.g., ASTM 992 steel), and the material was considered linear elastic, which should apply to most offshore structures. In this way, the nonlinear effects (that are expected to grow with the load magnitude) were assessed up to a reasonable value of the external actions on the structure. Note that a structure may suffer from buckling before this level of loading is reached; therefore, our calculations should encompass the likely expected loading conditions of supports for offshore turbines. Higher stresses would not be experienced by a reasonably designed structure and therefore, higher-than-assumed loads and their associated nonlinearities were ignored in this study.

Future studies will investigate the dynamic response in more detail, including other dynamic nonlinearities, hydrodynamic and inertial loading, and soil-structure interaction.

3. CASE STUDY I: MONOPILE

The monopile/tower support of this case study was modeled after the OC3 [13] configuration designed for the NREL 5-MW reference turbine [14] and for a 20-m water depth site. Main geometric parameters for this structure are shown in Table 1. The monopile was assumed clamped at the sea-bed, and as having a deck height of 10 m above mean sea level

(MSL), where the tower connected to the substructure. The tower was assumed linearly tapered in diameter and thickness.

The density of the steel was artificially augmented by 8% to 8,500 kg/m^3 to account for secondary steel, appurtenances, and coatings not included in the thickness data. The RNA was modeled as a lumped mass located at 2.34 m above the tower top and rigidly connected vertically above the tower-top cross section. For simplicity, RNA rotational inertia was not included. Figure 1 shows a three-dimensional rendering of this support structure while also showing the Von-Mises stresses as calculated by ANSYS for the larger-thrust static analysis introduced below.

Table 1. Monopile and tower geometric, inertial, and thrust parameters.

Parameter	*Value*
Deck height above MSL [m]	10
Monopile OD (outer diameter) [m]	6
Monopile wall thickness [m]	0.06
Tower-base OD [m]	6
Tower-base thickness [m]	0.027
Tower-top OD [m]	3.87
Tower-top thickness [m]	0.019
Tower length [m]	77.6
Turbine hub height above MSL [m]	90
RNA vertical offset [m]	2.34
Thrust [kN]	2,000 & 3,500
Assumed steel density [kg/m^3]	8,500
RNA mass [kg]	3.5E5
Monopile mass [kg]	285,580
Tower mass [kg]	237,093

A modal and a static analysis were performed to compare natural frequencies and tower deflections via GEBT, ANSYS, and SubDyn. The static analysis was run in both linear and nonlinear mode (except for SubDyn), and for the modal analysis, the effect of axial compression (due to self-weight) on the stiffness and frequency was checked with ANSYS.

For this study, GEBT used 120 beam elements. SubDyn used 120 Timoshenko elements equally subdivided between tower and monopile. ANSYS was initially run with 20 elements for both monopile and tower, and subsequently, with 60 and 100 elements in the tower to assess the effect on the calculated modes. There were no appreciable differences in the first 10 modes with errors less than 10^{-4} Hz. GEBT was also run with 30 and 60 elements in the tower portion and differences in calculated eigenfrequencies were on the order of 0.3%. A check was also performed on the support structural mass as calculated by all of the tools. Relative errors were less than 10^{-6} (fraction value).

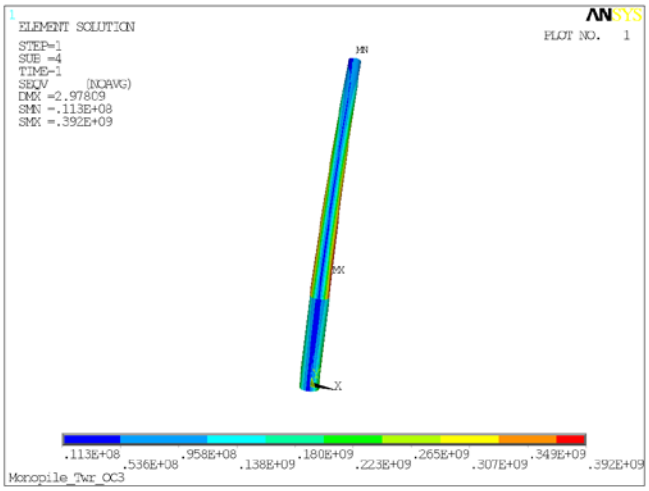

Figure 1. Von-Mises stresses [Pa] as calculated by ANSYS, for the nonlinear case with thrust=3,500 kN and downward force at the RNA of 3,500 kN.

There is no direct way to account for self-weight in GEBT and SubDyn during a modal analysis. When run with self-weight enabled, ANSYS showed a sensitivity of the first eigenfrequency to the number of elements of about 0.6% going from 20 to 100 elements in the tower. Overall, a 2% difference between the frequencies calculated with and without compression effects was also noted.

Modal analysis results from SubDyn, ANSYS and GEBT are compared in Table 2 and in graphic format in Figure 2.

Table 2. First 10 natural frequencies (in Hz) for the monopile support, as calculated by SubDyn, GEBT, and ANSYS. In parentheses is the percent difference with respect to the values calculated by ANSYS. The last column provides ANSYS results that include self-weight effects.

Mode		*SubDyn*	*GEBT*	*ANSYS*	*ANSYS w/ pre-stress*
No.	*Description*				
1	1st side-side bending	0.27973 (0.03%)	0.28588 (2.23%)	0.27965	0.27393 (-2.05%)
2	1st fore-aft bending	0.27973 (0.03%)	0.28588 (2.23%)	0.27965	0.27393 (-2.05%)
3	2nd side-side bending	2.26645 (0.09%)	2.31323 (2.16%)	2.2643	2.2555 (-0.39%)
4	2nd fore-aft bending	2.26645 (0.09%)	2.31323 (2.16%)	2.2643	2.2555 (-0.39%)
5	3rd side-side bending	5.89095 (0.16%)	5.99764 (1.97%)	5.8817	5.8716 (-0.17%)
6	3rd fore-aft bending	5.89095 (0.16%)	5.99764 (1.97%)	5.8817	5.8716 (-0.17%)
7	1st extensional	7.11123 (0.0%)	7.12704 (0.22%)	7.1112	7.111 (0.0%)
8	4th fore-aft bending	11.23268 (0.15%)	11.40337 (1.67%)	11.216	11.205 (-0.1%)
9	4th side-side bending	11.23268 (0.15%)	11.40338 (1.67%)	11.216	11.205 (-0.1%)
10	1st Shell mode	11.48672 (0.0%)	11.46018 (-0.23%)	11.487	11.486 (-0.01%)

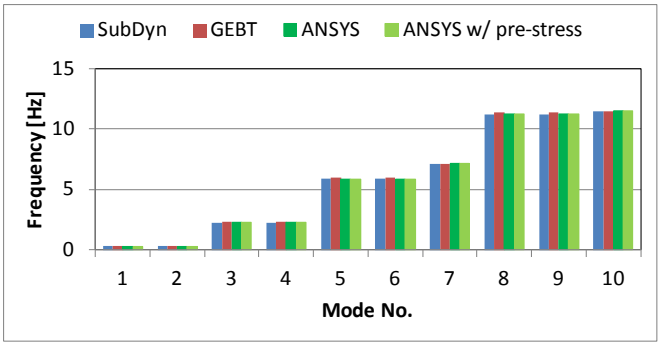

Figure 2. Graphic comparison of eigenfrequencies as calculated by the various tools for the monopile support.

There was general agreement in the output of the three software tools, and part of the differences is due to the way the RNA rigid connection is implemented. ANSYS can make use of constraint equations linking DOFs of the nodes of interest, whereas high stiffness/low density beam elements were used in the other tools.

Static analyses were performed under two rotor thrust loads (2,000 and 3,500 kN in magnitude) applied at the assumed RNA center of mass (CM) and directed along the horizontal x-axis. The steady-state thrust at rated power for the NREL 5-MW reference turbine is approximately 850 kN. Beside some level of conservatism, the assumed values of rotor thrust partially accounted for effects such as gusts and dynamic amplification. Additionally, the influence of the RNA self-weight was analyzed by adding a concentrated force (3,500 kN in magnitude) directed vertically downward and applied at the same RNA CM.

Table 3 provides results in terms of displacements along the direction of the thrust load as obtained by the software at the RNA CM and at the base of the tower. The same information is provided in graphic format in Figure 3.

Table 3. Deflections along the horizontal x-axis as calculated by SubDyn (linear calculations), and by GEBT and ANSYS (in linear and nonlinear modes), for the monopile/tower configuration.

Case	*Deflections at RNA [m]*				
Thrust/RNA-weight [kN]	SubDyn (Linear)	GEBT (Linear)	GEBT (Non-linear)	ANSYS (Linear)	ANSYS (Non-linear)
2,000/0	1.6445	1.6306	1.63	1.6443	1.6438
3,500/0	2.8778	2.8535	2.8505	2.8774	2.8748
2,000/3,500	1.6445	1.6306	1.693	1.6443	1.7035
3,500/3,500	2.8778	2.8535	2.9604	2.8774	2.9775
Case	*Deflections at Tower Base [m]*				
Thrust/RNA Weight [kN]	SubDyn (Linear)	GEBT (Linear)	GEBT (Non-linear)	ANSYS (Linear)	ANSYS (Non-linear)
2,000/0	0.08805	0.088	0.088	0.08805	0.08804
3,500/0	0.15409	0.1541	0.154	0.1541	0.15402
2,000/3,500	0.08805	0.088	0.0906	0.08805	0.0905
3,500/3,500	0.15409	0.1541	0.1584	0.1541	0.15822

Table 3 shows that, when no RNA weight effect is included, the difference in deflections is negligible between the linear and nonlinear approaches. The largest difference in tower-top deflections seen in the ANSYS results amounts to 0.1% under the larger thrust load.

With the RNA weight included, the linear calculations did not show any variations in terms of displacements along the x-axis, as one would expect. The ANSYS nonlinear results, however, showed a 3.5% (3.4%) increase in tower-top deflection when compared to their linear counterparts, under the higher (lower) thrust load. The deflections at the tower base followed a similar trend; when considering the effect of the tower-top weight, tower-base deflections increased by 2.7% and 2.6% for high and low thrust cases respectively. Analogous conclusions can be drawn from the GEBT data. Note that the largest difference in linear versus nonlinear deflections at the structure top is on the order of 10 cm.

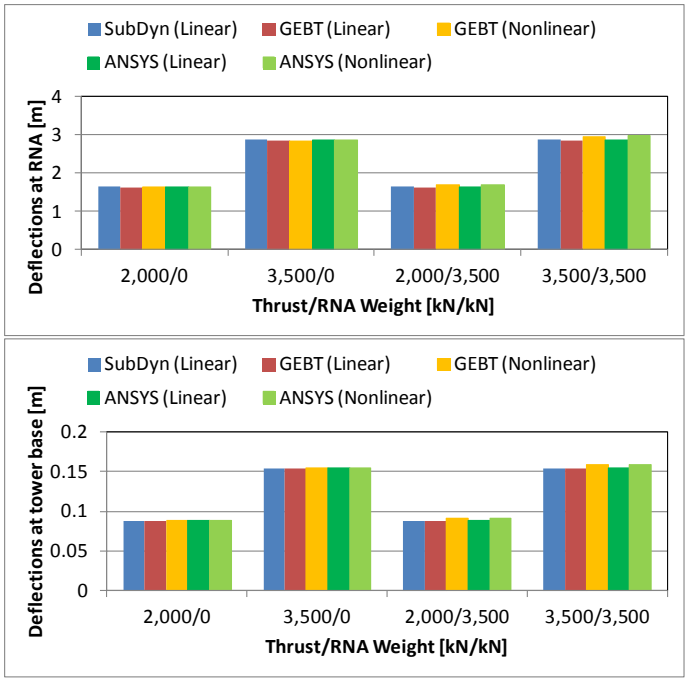

Figure 3. Graphic comparison of the deflections at the RNA location (top) and at the base of the tower (bottom) as calculated by the various tools for the monopile configuration.

One more analysis was conducted with ANSYS, where the self-weight of the tower and monopile was also included in a nonlinear static calculation under maximum thrust. Results showed that the tower-top deflection increase with respect to the weightless case rose to about 4% (from 3.5%). Note that this is equivalent to a P-Delta effect commonly investigated in civil structures through second-order analysis. These results indicated that our simplified approach, which only considered the RNA weight action, is applicable to assess nonlinear effects on static deflections for the monopile with negligible loss in accuracy.

4. CASE STUDY II: OC3 TRIPOD

The tripod is a hybrid structure between a monopile and a multimember jacket. A central column, similar to a monopile, connects to the tower via a transition piece at its top. At its bottom, the column connects to a space-frame, similar to a jacket, which transfers loads to three foundation piles below via pile-sleeves.

The example we discuss here is based on the OC3 tripod [13], a structure destined for a 45-m water-depth site, and the NREL 5-MW reference turbine. For the sake of expanding the cases and configurations analyzed, we slightly modified the RNA properties, and the base material density was set as in the previous case study to 8,500 kg/m^3.

The main geometric parameters are provided in Table 4. For simplicity, the transition piece is assumed to be a single member 4.5 m long with constant outer diameter (OD) and tapered thickness. The ~70-m long tower starts at 18 m above MSL and features a tapered OD and thickness. Figure 4 provides a three-dimensional rendering of the tripod and tower layout used in this study while also showing the Von-Mises stress field as calculated by ANSYS for one of the static load cases considered.

SubDyn, ANSYS, and GEBT were utilized to model this case. In the ANSYS discretization, each sub-member was simulated with 10 pipe elements, while the tower was modeled with 20 tapered beam elements; the central column was subdivided in tapered and nontapered segments, each represented by 10 beam elements. SubDyn and GEBT used 60 elements in the tower and 106 elements for the remainder of the structure (or approximately 2 elements per submember). Calculated masses matched pretty closely with a maximum relative difference of 10^{-5} among all three models.

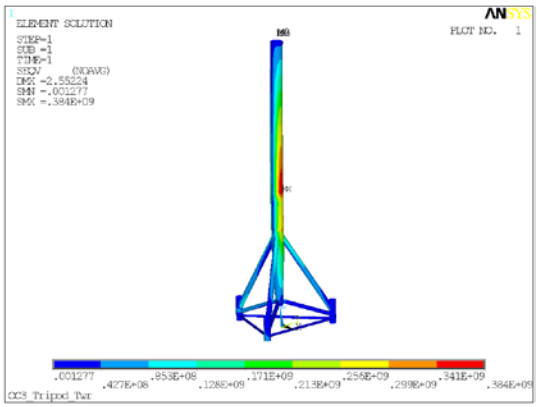

Figure 4. Von-Mises stresses [Pa] as calculated by ANSYS, for the nonlinear, static analysis of the tripod with high thrust, and RNA weight applied.

The derived eigenfrequencies are compared in Table 5 and Figure 5. ANSYS was also run in pre-stress mode to verify the effect of self-weight of the entire structure. Self-weight caused the first two mode frequencies to decrease by 2% to 3%, whereas modes 5 through 10 (mud-brace modes) showed an increase in frequency. This is likely due to the tension that developed in the mud braces under the weight action of the remainder of the support.

As a general comparison among the tools' results, Table 5 shows excellent agreement between ANSYS and SubDyn; GEBT estimated higher eigenfrequencies by 2% to 3%. The reason for these discrepancies in GEBT was not fully investigated.

Table 4. Tripod and tower geometric, inertial, and thrust parameters.

Parameter	*Value*
Deck height above MSL [m]	18
Sleeve OD [m]	3.15
Sleeve wall thickness [m]	0.035 (below mud-joint)-0.045
Mud-brace OD [m]	1.2
Mud-brace wall thickness [m]	0.025
Lower brace OD [m]	1.875
Lower brace wall thickness [m]	0.025
Upper brace OD [m]	2.475
Upper brace wall thickness [m]	0.035
Central column taper section OD [m]	3.14 (bottom)-5.7 (top)
Central column Taper Section thickness [m]	0.05
Central column constant-OD section [m]	5.7
Central column constant-OD section thickness [m]	0.05
Transition-Piece OD [m]	5.7
Transition-Piece (TP) thickness [m]	0.05-0.032
Tower-base OD [m]	5.7
Tower-base thickness [m]	0.032
Tower-top OD [m]	5.51
Tower-top thickness [m]	0.024
Tower length [m]	69.6
Turbine hub height [m]	90
RNA vertical offset [m]	2.34
RNA mass [kg]	574,000(*)
Tripod +TP mass [kg]	983,675
Tower mass [kg]	290,269
Thrust [kN]	2,000 & 4,000

(*) RNA mass arbitrarily changed from the NREL 5- MW's to represent a larger turbine on top of this support.

As in the previous case study, we subjected the structure to two levels of rotor thrust load (2,000 and 4,000 kN) applied at the location of the RNA and directed along the x-axis, parallel to one of the three sides of the tripod base. In Figure 4, the Von-Mises stress field exhibits a limited plastic region (stresses higher than 345 MPa) under the higher thrust case. The calculated deflections at tower top and base are given in Table 6 and in graphic format in Figure 6. There is very good agreement in the results from the various tools, with relative errors among analogous calculations of less than 0.1%.

Static simulations with applied thrust loads were repeated by including the RNA weight as a concentrated force (5,738

kN) applied at the RNA CM location. Results are also provided in Table 6.

When the RNA weight is excluded, differences in deflection values between linear and nonlinear cases are negligible (<0.1%). The weight load has no appreciable effect on the linearly computed deflections; however, deflections increased by about 4% (3.5%) at the tower-top (base) when a nonlinear approach was used. These differences amount to about 10 cm at the tower top and 1 cm at the tower base.

Table 5. Tripod support first 10 natural frequencies (in Hz) as calculated by SubDyn, GEBT, and ANSYS. In parentheses is the percent difference with respect to the ANSYS calculated values. The last column provides ANSYS results that include self-weight effects.

Mode		*SubDyn*	*GEBT*	*ANSYS*	*ANSYS w/ pre-stress*
No.	*Description*				
1	1st side-side bending	0.25231 (0.06%)	0.25631 (1.64%)	0.25217	0.24596 (-2.46%)
2	1st fore-aft bending	0.25231 (0.06%)	0.25631 (1.64%)	0.25217	0.24596 (-2.46%)
3	2nd side-side bending	2.5042 (0.14%)	2.55048 (1.99%)	2.5007	2.4918 (-0.36%)
4	2nd fore-aft bending	2.5042 (0.14%)	2.55044 (1.99%)	2.5007	2.4919 (-0.35%)
5	1st mud-brace bending, horizontal plane	3.88801 (0.13%)	4.02359 (3.62%)	3.8829	3.8952 (0.32%)
6	2nd mud-brace bending, horizontal plane	3.88812 (0.13%)	4.02575 (3.68%)	3.883	3.8953 (0.32%)
7	1st mud-brace bending, vertical plane	3.9008 (0.13%)	4.03766 (3.64%)	3.8959	3.9081 (0.31%)
8	2nd mud-brace bending, vertical plane	3.91987 (0.13%)	4.05753 (3.65%)	3.9148	3.9271 (0.31%)
9	3rd mud-brace bending, vertical plane	3.91999 (0.13%)	4.05831 (3.66%)	3.915	3.9272 (0.31%)
10	3rd mud-brace bending, horizontal plane	3.94016 (0.13%)	4.0783 (3.64%)	3.935	3.9474 (0.32%)

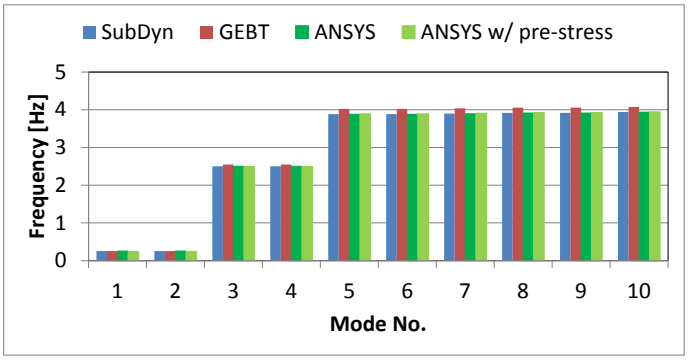

Figure 5. Eigenfrequencies as compared in Table 5, but in graphic format.

Table 6. Deflections along the horizontal x-axis as calculated by SubDyn (linear calculations), and by GEBT and ANSYS (in linear and nonlinear modes), for the OC3 tripod/tower configuration.

Case	*Deflections at RNA [m]*				
Thrust/RNA Weight [kN]	SubDyn (Linear)	GEBT (Linear)	GEBT (Non-linear)	ANSYS (Linear)	ANSYS (Non-linear)
2,000/0	1.22238	1.22194	1.22170	1.2237	1.2235
4,000/0	2.44477	2.44389	2.44211	2.4475	2.4458
2,000/5,738	1.22238	1.22194	1.27734	1.2237	1.2766
4,000/5,738	2.44477	2.44389	2.55318	2.4475	2.5518
Case	*Deflections at Tower Base [m]*				
Thrust/RNA Weight [kN]	SubDyn (Linear)	GEBT (Linear)	GEBT (Non-linear)	ANSYS (Linear)	ANSYS (Non-linear)
2,000/0	0.11416	0.11486	0.11484	0.11443	0.11441
4,000/0	0.22833	0.22972	0.22960	0.22887	0.22875
2,000/5,738	0.11416	0.11486	0.11946	0.11443	0.11861
4,000/5,738	0.22833	0.22972	0.23883	0.22887	0.23714

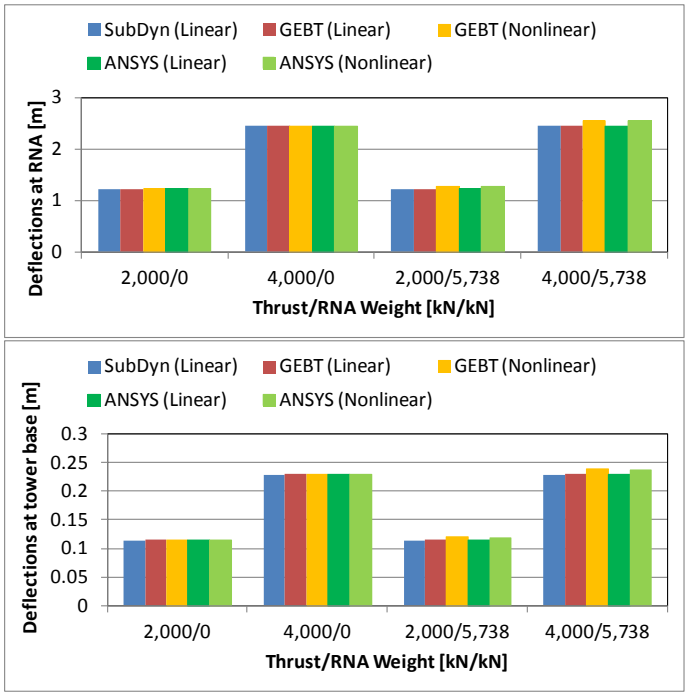

Figure 6. Graphic comparison of the deflections at the RNA location (top) and at the base of the tower (bottom) as calculated by the various tools for the OC3 tripod/tower configuration.

5. CASE STUDY III: OC4 JACKET

For this example, we analyzed a jacket designed to support the NREL 5-MW reference turbine as used in the OC4 research project [15]. This support layout is designed for systems to be deployed at sites with 50-m water depth. Its main geometric parameters are provided in Table 7, and more details can be found in [16].

The jacket-tower support structure was modeled in SubDyn and ANSYS. GEBT did not yield reliable results, most likely because of the way the transition piece was modeled. The transition piece was simulated with either a very stiff frame of beams (GEBT and SubDyn) or with perfectly rigid connections (ANSYS). In each model, the transition piece mass was represented by a lumped mass (including rotational inertia) located at the half transition-piece length. GEBT provided spurious results when trying to simulate the rigid connection between tower and jacket, therefore GEBT results for this and other jacket/tower layouts were not included in this paper.

In the ANSYS model, five pipe elements were utilized per jacket member and 20 tapered beam elements for the tower. SubDyn used 160 elements for the tower and 258 elements for the remainder of the jacket structure with approximately two elements per member. The steel density was artificially augmented to 8,500 kg/m^3, namely to account for secondary steel. The maximum relative difference in calculated mass between the ANSYS and SubDyn models was less than 6×10^{-4}.

Figure 7 provides a general three-dimensional rendering of the structure (the third eigenmode shape is shown in the figure) (the transition piece is not shown). Note that the piles were truncated at the sea-bed, where they were assumed as perfectly clamped. In the original jacket configuration design [15], the jacket legs were grouted within the piles. We approximated this connection by simplistically increasing the pile wall thickness. Although this approximation artificially raises the overall structural stiffness, a separate ANSYS calculation proved that by ignoring the grout altogether, and considering a simple joint with the leg at the pile head, the conclusions of this study did not change (see columns with asterisks in Table 8 and Table 9).

Table 7. OC4 jacket and tower geometric, inertial, and thrust parameters.

Parameter	*Value*
Deck height above MSL [m]	16
Transition-piece length [m]	4
Tower-base OD [m]	5.6
Tower-base thickness [m]	0.032
Tower-top OD [m]	4
Tower-top thickness [m]	0.03
Tower length [m]	68
Leg OD	1.2
Leg thickness [m]	0.05(up to 1st bay)-0.035-0.04 (TP)
Brace OD [m]	0.8
Brace thickness [m]	0.02
Pile OD [m]	2.082
Pile thickness [m]	0.6
RNA vertical offset [m]	2.34
Turbine hub height [m]	90
RNA mass [kg]	350,000
Jacket mass [kg]	581,256+(427,174 pile/grout)
Transition piece mass [kg]	666,000
Tower mass [kg]	229,812
Thrust [kN]	2,000 & 4,000

Table 8 and Figure 8 provide a comparison between the first 10 natural frequencies as calculated by ANSYS and SubDyn. There is good agreement in the data with relative errors on the order of 0.1% or less, except for mode 5, which is a torsion mode where the discrepancy between the calculated values is on the order of 2%. This may be a result of the different approximations used in the modeling of the transition piece and piles. Also from Table 8, it can be seen that the self-weight effect reduces the first two eigenfrequencies by 1.5%. The simplified grouting modeling had a 2% to 18% impact on the mode frequencies, with the largest effect on the fifth mode frequency. Nonetheless, the SubDyn model produced very consistent results when compared to ANSYS, even with this geometric configuration.

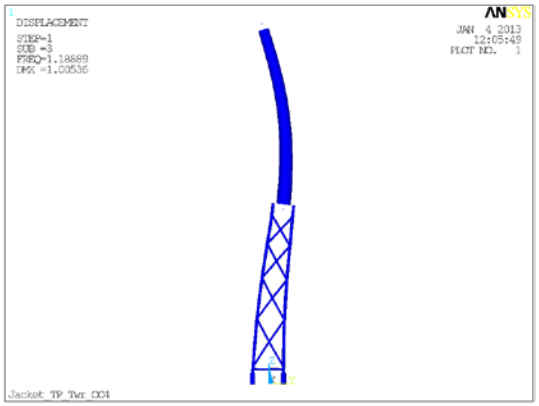

Figure 7. Third mode as calculated by ANSYS for the OC4 jacket-tower support configuration.

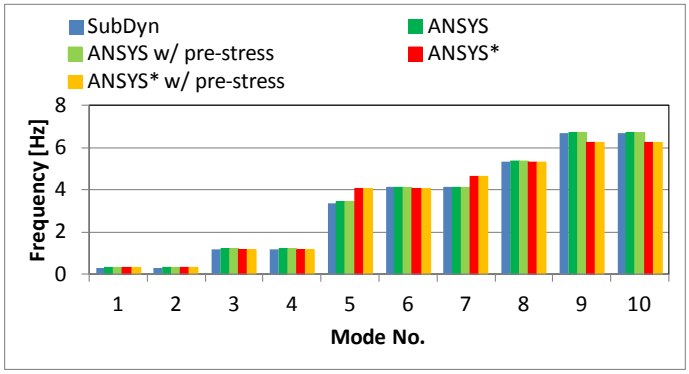

Figure 8. Graphic comparison of eigenfrequencies as calculated by the various tools for the OC4 support. The "*" symbols denote calculations' results that ignored grouted connections.

Static analyses were performed under two rotor thrust loading levels: 2,000 and 4,000 kN. Figure 10 shows the calculated Von-Mises stresses under the larger thrust load as computed by ANSYS. These thrust values, as done previously, should encompass the expected range of maximum loading conditions for the turbine support. The thrust vector, applied at the RNA CM, was assumed as being aligned along the diagonal

of the jacket base to simulate a worst-case scenario for the legs and piles. ANSYS was run in both linear and nonlinear mode and tower-top and tower-base deflections are compared to SubDyn's data in Table 9 and Figure 9.

It can be seen from the table that linearly calculated deflections agree within 0.05% between SubDyn and ANSYS, and that, as expected, the RNA weight does not change those results. With no RNA weight included, the nonlinearities are below 0.1% (relative error in calculated deflections). Under the effect of RNA weight, however, differences are on the order of 3% and 2%, or less than 6 cm and 1 cm at tower top and tower base respectively.

Of note is the role played by the piles and the assumed connection to the legs. When the grouting is ignored, differences in calculated deflections between linear and nonlinear treatments are comparable to those seen with a simplified representation of the grout. Thus, the connection at the base of the jacket between pile and legs may not be critical in terms of nonlinearities. Yet, the soil-pile interaction is nonlinear in nature, and a future soil module to pair with SubDyn will need to account for that. This aspect, however, is beyond the scope of this paper.

Table 8. OC4 support first 10 eigenfrequencies (Hz) as calculated by SubDyn and ANSYS. In parentheses is the percent difference with respect to the ANSYS calculated values. Columns labels as "w/pre-stress" provide results including the effect of structure self-weight.

Mode		*SubDyn*	*ANSYS*	*ANSYS w/ pre-stress*	*ANSYS(*)*	*ANSYS w/ pre-stress(*)*
No.	*Description*					
1	1st side-side bending	0.31897 (0.0%)	0.31896	0.31404 (-1.54%)	0.31674 (-0.7%)	0.31185 (-2.23%)
2	1st fore-aft bending	0.31897 (0.0%)	0.31896	0.31404 (-1.54%)	0.31674 (-0.7%)	0.31185 (-2.23%)
3	2nd side-side bending	1.19283 (-0.06%)	1.1936	1.1889 (-0.39%)	1.1613 (-2.71%)	1.1565 (-3.11%)
4	2nd fore-aft bending	1.19284 (-0.06%)	1.1936	1.1889 (-0.39%)	1.1613 (-2.71%)	1.1565 (-3.11%)
5	1st torsional	3.38381 (-1.7%)	3.4425	3.4397 (-0.08%)	4.0788 (18.48%)	4.0693 (18.21%)
6	3rd fore-aft bending	4.12416 (-0.03%)	4.1253	4.1159 (-0.23%)	4.0788 (-1.13%)	4.0693 (-1.36%)
7	3rd side-side bending	4.12417 (-0.03%)	4.1253	4.1159 (-0.23%)	4.6346 (12.35%)	4.6297 (12.23%)
8	1st extensional	5.33918 (0.0%)	5.3391	5.3385 (-0.01%)	5.286 (-0.99%)	5.2853 (-1.01%)
9	4th side-side bending +brace mode	6.68688 (-0.13%)	6.6953	6.6857 (-0.14%)	6.2539 (-6.59%)	6.2429 (-6.76%)
10	4th fore-aft bending +brace mode	6.68688 (-0.13%)	6.6953	6.6857 (-0.14%)	6.2539 (-6.59%)	6.2429 (-6.76%)

(*) Calculations ignored grouted connection

Table 9. Deflections at the RNA location and at the tower base as calculated by SubDyn and ANSYS for the OC4 jacket/tower configuration.

Case	*Deflections at RNA [m]*				
Thrust/RNA Weight [kN]	SubDyn (Linear)	ANSYS (Linear)	ANSYS (Non-linear)	ANSYS (Linear) (*)	ANSYS (Non-linear) (*)
2,000/0	1.20834	1.20890	1.20870	1.2219	1.2217
4,000/0	2.41669	2.4178	2.4161	2.4438	2.4421
2,000/3,500	1.20834	1.2089	1.2408	1.2219	1.2533
4,000/3,500	2.41669	2.4178	2.4802	2.4438	2.507

Case	*Deflections at Tower Base [m]*				
Thrust/RNA Weight [kN]	SubDyn (Linear)	ANSYS (Linear)	ANSYS (Non-linear)	ANSYS (Linear) (*)	ANSYS (Non-linear) (*)
2,000/0	0.13750	0.1375	0.1374	0.14405	0.14403
4,000/0	0.27500	0.2749	0.2748	0.28809	0.28794
2,000/3,500	0.13750	0.1375	0.1398	0.14406	0.14645
4,000/3,500	0.27500	0.2749	0.2795	0.28810	0.29287

(*) Calculations ignored grouted connection

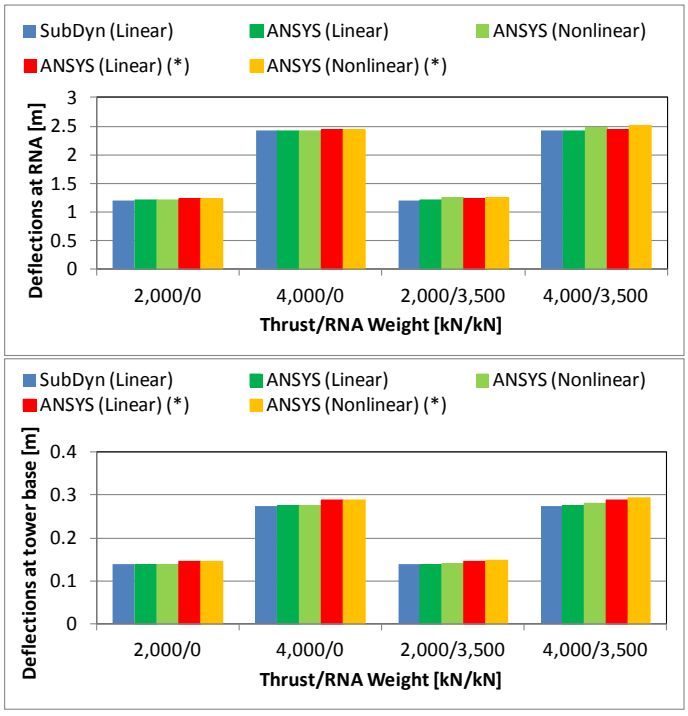

Figure 9. Graphic comparison of the deflections at the RNA location (top) and at the base of the tower (bottom) as calculated by the various tools for the OC4 support configuration. The (*) symbols denote calculations that ignored grouted connections.

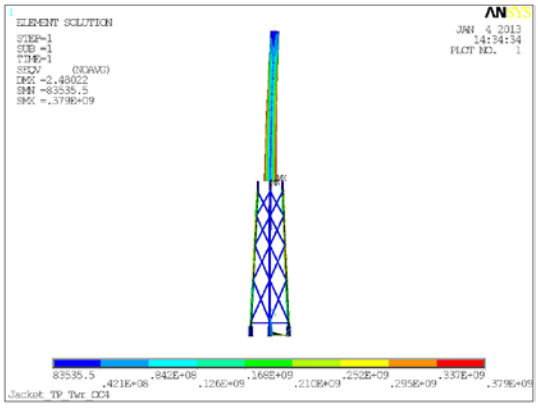

Figure 10. Von-Mises stresses [Pa] as calculated by ANSYS, for the nonlinear, static analysis of the OC4 support with high thrust, and RNA weight applied.

6. CASE STUDY IV: 7-MW TURBINE JACKET

In this example, we investigated the possible nonlinearities associated with a support for a 7-MW wind turbine with a hub-height of about 100 m. This is a jacket/tower configuration designed for a 40-m water-depth that features four levels of X-bracings in addition to horizontal braces (see also Figure 11 for a three-dimensional rendering of the structure). In contrast to the previous jacket example, the angle between braces and legs changes from bay to bay, and the bay height is kept constant. Other geometric parameters are provided in Table 10. In this study, the batter is defined as the tangent of the lesser angle between the leg direction and the horizontal in a two-dimensional elevation projection. Analogous to the OC4 jacket, the transition piece was assumed to be made of a reinforced concrete block of mass equal to 666 tonnes. The jacket was assumed perfectly clamped at the leg feet on the seabed with mud braces at 4 m above the seabed. As in the previous example, given the difficulties associated with the rigid transition-piece modeling in GEBT, only the results of analyses performed via SubDyn and ANSYS are included.

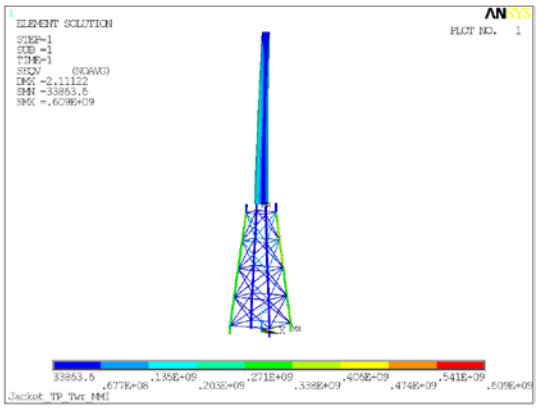

Figure 11. Three-dimensional rendering of the support structure showing Von-Mises stresses [Pa] as calculated by ANSYS, for the nonlinear, static analysis of the 7-MW turbine support with high thrust, and RNA weight applied.

In ANSYS, the tower was simulated with 20 tapered elements, and with10 elements per member in the remainder of the support structure. SubDyn utilized 180 elements in the tower and 242 elements for the jacket members (approximately two elements per member). The relative difference in structural mass as calculated by the two models was within 10^{-5}.

Table 10. 7-MW jacket/tower geometric, inertial, and thrust parameters.

Parameter	*Value*
Deck height above MSL [m]	15
Jacket batter [-]	10
Leg OD [m]	1
Leg wall thickness [m]	0.021
Brace OD [m]	0.4
Brace wall thickness [m]	0.011
Tower-base OD [m]	6.4
Tower-base thickness [m]	0.053
Tower-top OD [m]	3.52
Tower-top thickness [m]	0.029
Tower length [m]	78
RNA vertical offset [m]	2.34
Turbine hub height [m]	100
RNA mass [kg]	515,000
Jacket mass [kg]	237,971
TP mass [kg]	666,000
Tower mass [kg]	435,454
Thrust [kN]	2,000 & 4,000

As in the previous examples, modal analyses were conducted and the obtained first 10 eigenfrequencies are shown in Figure 12 and Table 11. SubDyn and ANSYS results matched very well (relative errors below 0.6%) when the effect of self-weight was ignored, which amounted to about 2%.

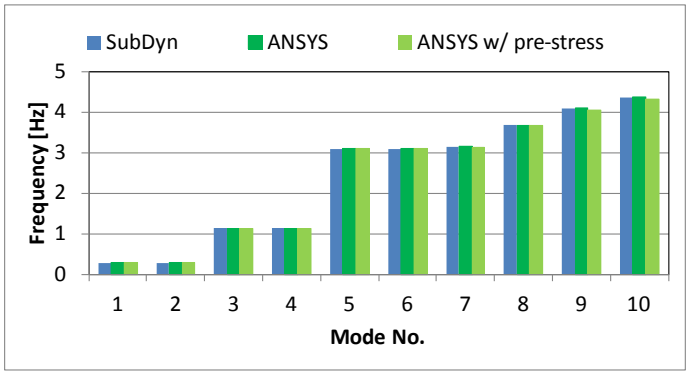

Figure 12. Graphic comparison of eigenfrequencies as calculated by the various tools for the 7-MW turbine support.

Static analyses were performed to assess deflections at the RNA and at the tower base under two levels of rotor thrust loading (2,000 kN and 4,000 kN), and considering the RNA-weight effect as a concentrated force along the vertical. The assumed thrust vector and displacements were directed along the diagonal of the jacket base. In Table 12 and Figure 13, the

deflections at tower top and tower base are provided as calculated by the two tools. The linear solutions matched within 1% between ANSYS and SubDyn, and the RNA weight had no appreciable effect on the results (only differences were due to round-off errors). When ANSYS was run in nonlinear mode and with no RNA weight included, maximum relative differences in the deflections with respect to the linear cases amounted to 1% (as in the case of SubDyn). These differences increased to about 2% for tower-base deflections and between 2% to 3% for tower-top deflections when the RNA weight was included. The absolute difference in displacement between the linear and nonlinear approaches was within 6 cm at the tower top and less than 1 cm at the tower base.

Table 11. First 10 natural frequencies (in Hz) as calculated by SubDyn and ANSYS for the 7-MW support structure. The last column provides results that include the effect of structure self-weight.

Mode		*SubDyn*	*ANSYS*	*ANSYS w/ pre-stress*
No.	*Description*			
1	1st fore-aft bending	0.28491 (-0.44%)	0.28618	0.28127 (-1.72%)
2	1st side-side bending	0.28491 (-0.44%)	0.28618	0.28127 (-1.72%)
3	2nd fore-aft bending	1.13387 (0.0%)	1.1339	1.1281 (-0.51%)
4	2nd side-side bending	1.13387 (0.0%)	1.1339	1.1281 (-0.51%)
5	3rd fore-aft bending +brace	3.07957 (-0.57%)	3.0971	3.086 (-0.36%)
6	3rd side-side bending +brace	3.07957 (-0.57%)	3.0971	3.086 (-0.36%)
7	1st torsional	3.14491 (-0.01%)	3.1453	3.137 (-0.26%)
8	1st extensional	3.6681 (-0.24%)	3.677	3.6763 (-0.02%)
9	1st brace local mode	4.09176 (0.17%)	4.0849	4.0385 (-1.14%)
10	2nd brace local mode	4.36419 (0.17%)	4.357	4.3086 (-1.11%)

Table 12. Deflections at the RNA location and at the tower base as calculated by SubDyn and ANSYS for the 7-MW jacket/tower configuration.

Case	*Deflections at RNA [m]*		
Thrust/RNA Weight [kN]	SubDyn (Linear)	ANSYS (Linear)	ANSYS (Non-linear)
2,000/0	1.03484	1.02580	1.02320
4,000/0	2.06967	2.05150	2.05060
2,000/5,150	1.03484	1.02580	1.05380
4,000/5,150	2.06967	2.05160	2.11120
Case	*Deflections at Tower Base [m]*		
Thrust/RNA Weight [kN]	SubDyn (Linear)	ANSYS (Linear)	ANSYS (Non-linear)
2,000/0	0.10737	0.10742	0.10729
4,000/0	0.21474	0.21483	0.21481
2,000/5,150	0.10737	0.10754	0.10933
4,000/5,150	0.21474	0.21489	0.21869

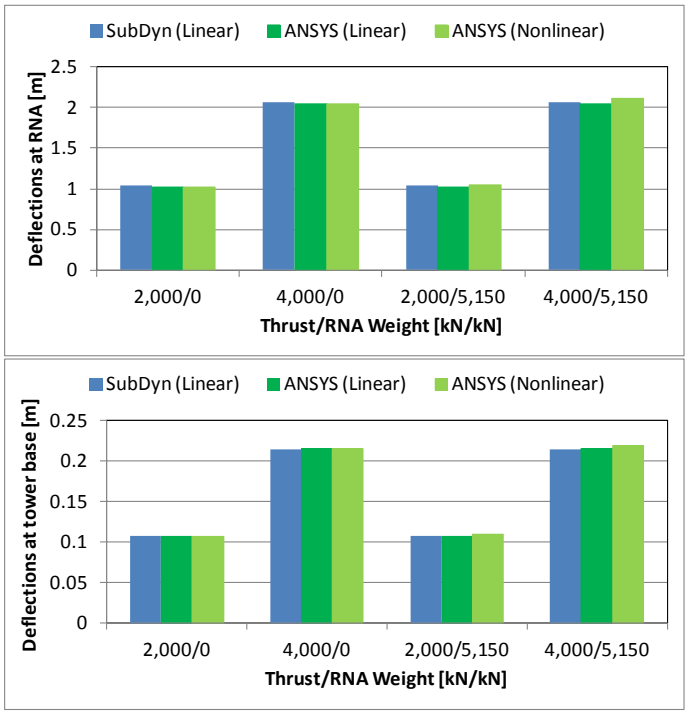

Figure 13. Graphic comparison of the deflections at the RNA location (top) and at the base of the tower (bottom) as calculated by the various tools for the 7-MW turbine support configuration.

7. CASE STUDY V: 10-MW TURBINE JACKET

To conclude this gallery of jacket/tower configuration case studies, we investigated a large support structure designed for a 10-MW turbine. Some information on the basic design of this support and turbine attributes can be found in [17], and main geometric parameters are provided in Table 13. The jacket is stiffened by four levels of X-bracings, and the interface with the tower occurs at about 16 m above MSL through an all-steel transition piece. The transition piece is envisioned as a stringer-reinforced deck supporting a central cylindrical shell supported by four tubular struts. The piles are intended to be driven through the legs and thus feature a batter angle as well.

This model was examined via ANSYS alone, where five elements per member were used for the jacket, the tower was modeled with 24 tapered elements, and 12 elements were used for the piles. The soil-pile interaction was approximated through nonlinear spring elements implemented through API p-y relationships [18] at each pile node. The first fourth of the tower was at constant diameter and thickness. SubDyn has not been paired to a soil module yet, and it does not include shell elements to simulate a deck as in the present case. Thus, it was not employed in this example.

Worth noticing is the presence of a horizontal offset for the RNA CM in this case that led to a gravity moment at the tower top. In the other examples in this study, RNA horizontal offsets were ignored. A three-dimensional view of the support is

offered in Figure 14 that also shows the equivalent stress field obtained as a result of the static analysis described below.

Table 13. 10-MW jacket/tower geometric, inertial, and thrust parameters.

Parameter	*Value*
Deck height above MSL [m]	16
Jacket batter [-]	8.47
Leg OD [m]	1.74
Leg wall thickness [m]	0.029
Brace (mud-brace) OD [m]	0.61(0.762)
Brace (mud-brace) wall thickness [m]	0.016(0.0174)
Tower-base OD [m]	7
Tower-base thickness [m]	0.055
Tower-top OD [m]	3.85
Tower-top thickness [m]	0.03
Tower length [m]	88.4
Turbine hub height [m]	116
RNA horizontal offset [m]	4.81
RNA vertical offset [m]	3.05
RNA mass [kg]	1,072,000
Jacket mass [kg]	615,000
TP mass [kg]	300,000
Tower mass [kg]	639,535
Thrust [kN]	3400

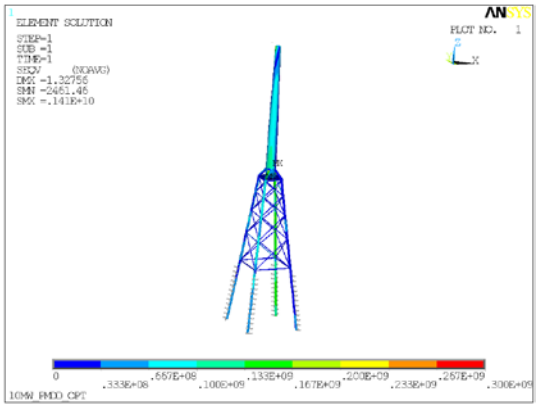

Figure 14. Von-Mises stresses [Pa] as calculated by ANSYS, for the nonlinear, static analysis of the 10-MW turbine support with high thrust and RNA weight applied.

For completeness, the calculated mode frequencies are shown in Figure 15 and Table 14, and they include the effect of self-weight of the entire structure.

In the static analysis, besides the action of structure self-weight, the support was subjected to a thrust load of 3,400 kN directed along the diagonal of the jacket base and applied at the assumed RNA CM. This loading setup resembled a yaw error situation and produced an additional torsional moment at the tower top, for, as mentioned, the CM was horizontally offset from the tower centerline. The load magnitude was left at one level, associated with the maximum expected thrust accounting for dynamic amplification and gust effects. ANSYS was run in both linear and nonlinear modes, and the results in terms of deflections obtained at the tower top and base are provided in Table 15 and Figure 16.

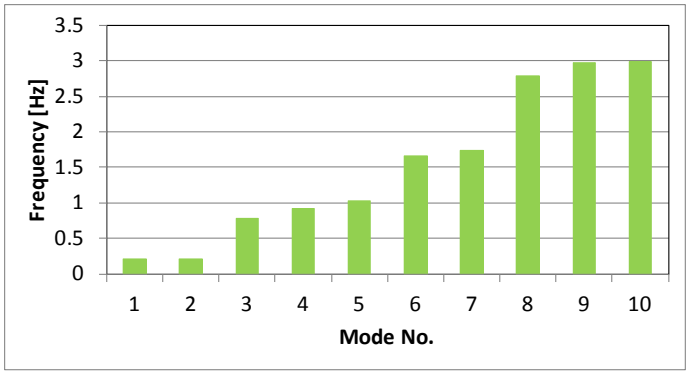

Figure 15. First 10 eigenfrequencies as calculated by ANSYS for the 10-MW support structure.

Table 14. First 10 natural frequencies (in Hz) as calculated by ANSYS accounting for self-weight of the entire structure.

Mode		*ANSYS w/ pre-stress*
No.	*Description*	
1	1st side-side bending	0.21320
2	1st fore-aft bending	0.21629
3	1st torsional	0.77688
4	2nd side-side bending	0.92634
5	2nd fore-aft bending	1.0313
6	3rd side-side bending +brace	1.6561
7	3rd fore-aft bending +brace	1.7426
8	1st brace local mode	2.7845
9	2nd brace local mode	2.9784
10	3rd brace local mode	2.9847

Relative differences in deflections as obtained through linear and nonlinear simulations amounted to about 5% at the tower top and 2% at the tower base. These differences, when translated to absolute values, amount to 6 cm at the tower top and 1 cm at the tower base.

Table 15. Deflections at the RNA location and at the base of the tower as calculated by ANSYS for the 10-MW support configuration.

Case	*Deflections at RNA [m]*	
Thrust/Weight [kN]	ANSYS (Linear)	ANSYS (Nonlinear)
3,400/entire structure self-weight	1.2688	1.3276
Case	*Deflections at Tower Base [m]*	
Thrust/Weight [kN]	ANSYS (Linear)	ANSYS (Nonlinear)
3,400/ self-weight	1.6639E-01	1.7039E-01

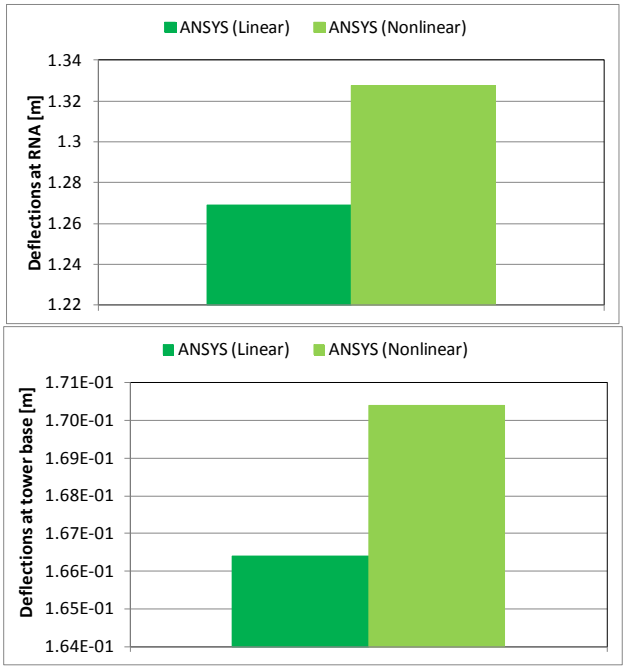

Figure 16. Graphic comparison of the deflections at the RNA location (top) and at the base of the tower (bottom) as calculated by ANSYS for the 10-MW support configuration.

8. CASE STUDY VI: ALL-LATTICE TOWER

Given the constraints on the modal performance of large offshore wind supports, the coupled jacket/tower configuration may not be the most economical, and an all-lattice support structure could be devised. This type of layout would also simplify the design of the transition piece, as the loads to be transferred from the yaw bearing (the bending moment in particular) would be almost one to two orders of magnitude lower than if the transition piece were located at the bottom of the tower. In this example, we simulated a three-legged lattice to support the NREL 5-MW turbine at a 30-m water-depth site consistent with a design proposed in [19]. The hub-height is assumed at 82 m above MSL, and the structure is designed with 10 levels of constant-angle X-bracings, including horizontal braces at every level. Other geometric parameters are given in Table 16.

Table 16. Three-legged lattice geometric, inertial, and thrust parameters.

Parameter	*Value*
Leg OD [m]	0.68
Leg wall thickness [m]	0.015
Brace OD [m]	0.272
Brace wall thickness [m]	0.006
Jacket batter [-]	13.83
Turbine hub height [m]	82
RNA vertical offset [m]	2.34
RNA mass [kg]	350,000
Lattice tower mass [kg]	144,500
Thrust [kN]	2,000 & 3,000

As done in the previous examples, the steel density was increased (8,500 kg/m^3) to account for secondary steel, coating, sacrificial anodes, etc. The structure was assumed clamped at the seabed, and the RNA was located some 2.3 m above the top level of bracing.

Both ANSYS and SubDyn were used to simulate this support. ANSYS used 10 elements per member; SubDyn utilized 376 elements in total, or two per member. The structural mass calculated by the two programs matched very closely with a relative error of about 6×10^{-5}. In Figure 17, a three-dimensional view of the structure is provided, which also shows deformed shape and Von-Mises stresses as calculated by ANSYS under one of the static load cases analyzed in this study.

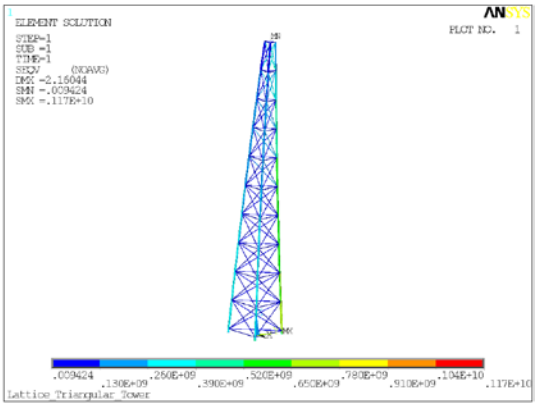

Figure 17. Von-Mises stresses [Pa] as calculated by ANSYS with a nonlinear run for the case of high-thrust and RNA weight as concentrated force at the RNA CM for the three-legged support.

The first 10 natural frequencies calculated by the two tools are provided in Table 17 and Figure 18.

Relative errors in eigenfrequencies are on the order of 1.6%, which is comparable to the effect of self-weight.

A static analysis was performed by assuming the turbine rotor thrust load vector as applied at the RNA CM and directed perpendicularly to one of the three sides. Two magnitudes for this load were considered (2,000 and 3,000 kN), which, as explained in the previous sections, should include the maximum load values to be encountered by this support. This structure is extremely light and likely would need some reinforcement for a realistic application; nonetheless, we still considered a maximum thrust load of 3,000 kN that resulted in a large region of stresses above yield (~345 MPa, see also Figure 17).

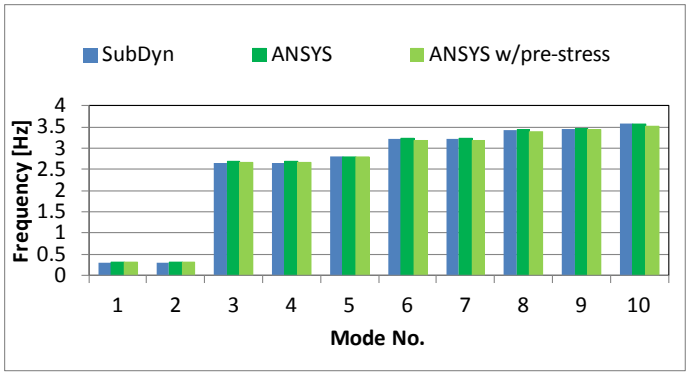

Figure 18. Graphic comparison of eigenfrequencies as calculated by the various tools for the all-lattice support.

Table 17. First 10 natural frequencies as calculated by SubDyn and ANSYS for the all-lattice structure.

Mode		*SubDyn*	*ANSYS*	*ANSYS w/ pre-stress*
No.	*Description*			
1	1st fore-aft bending	0.30575 (-1.6%)	0.31073	0.30578 (-1.59%)
2	1st side-side bending	0.30575 (-1.6%)	0.31073	0.30578 (-1.59%)
3	2nd fore-aft bending +brace	2.6621 (-0.82%)	2.6841	2.6667 (-0.65%)
4	2nd side-side bending +brace	2.6621 (-0.82%)	2.6841	2.6667 (-0.65%)
5	1st torsional	2.796 (0.04%)	2.795	2.7845 (-0.38%)
6	1st brace local mode	3.2331 (-0.02%)	3.2337	3.1744 (-1.83%)
7	2nd brace local mode	3.2331 (-0.02%)	3.2337	3.1744 (-1.83%)
8	1st extensional	3.4393 (-0.07%)	3.4418	3.3846 (-1.66%)
9	3rd brace local mode	3.461 (0.14%)	3.456	3.442 (-0.41%)
10	4th brace local mode	3.5758 (0.05%)	3.5739	3.5113 (-1.75%)

Results of the static analysis are given in Table 18 and in graphic format in Figure 19. Note that similarly to what was done in the previous cases, the weight of the RNA was accounted for via a concentrated downward force of 3,500 kN. The structure self-weight was ignored for simplicity.

Table 18. Deflections at the RNA location as calculated by ANSYS and SubDyn for the three-legged tower configuration.

Case	*Deflections at RNA [m]*		
Thrust/RNA Weight [kN]	SubDyn (Linear)	ANSYS (Linear)	ANSYS (Nonlinear)
2,000/0	1.3988	1.4035	1.4004
3,000/0	2.0982	2.1053	2.0978
2,000/3,500	1.3988	1.4035	1.442
3,000/3,500	2.0982	2.1053	2.1599

Excellent agreement is found between the two codes when run in linear mode (0.3% relative errors). Nonlinearities only appear associated with the effect of the RNA weight, or the P-Delta effect. A 3% maximum difference in the calculated deflections (or some 5 cm) can be seen under both thrust levels.

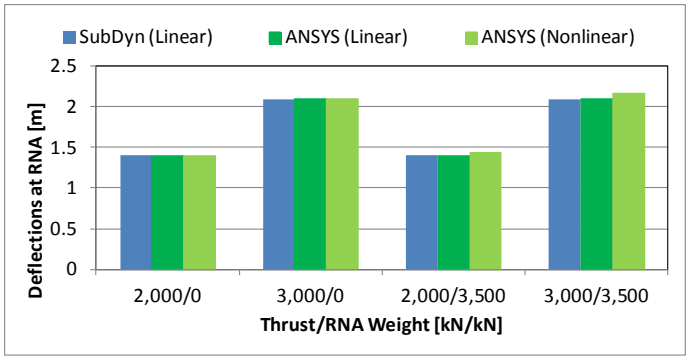

Figure 19. Graphic comparison of the deflections calculated at the RNA locations as calculated by SubDyn and ANSYS for the three-legged tower configuration.

9. CONCLUSIONS

A large portion of offshore wind power costs originate from the turbine support, particularly from the substructure of fixed-bottom configurations. It is crucial to control those costs through innovative and economically efficient designs. The certification-driven design process of a turbine requires sophisticated loads-analysis simulations that encompass a vast set of environmental conditions and operational scenarios. CAE tools, such as the NREL-developed FAST tool, are required to run efficiently on typical workstations to help in the design process while maintaining a high degree of fidelity in the physical representation of the entire system. This study introduced a new module for the aero-hydro-servo-elastic simulation of offshore wind turbines.

SubDyn is a module for the structural dynamics of offshore multimember substructures that makes use of a linear FEM pre-processor and a Craig-Bampton reduction approach, and which is totally integrated within the new FAST modularization framework. While this technique allows FAST/SubDyn to maintain high computational efficiency, one must prove that the neglected nonlinear effects are not important in the simulation of fixed-bottom supports. This study was used to determine whether it was sufficient to base SubDyn on a linear formulation. Nonlinear effects include: large displacements, axial shortening due to bending, cross-sectional transverse shear effects, etc. A nonlinear structural analysis of the substructure is computationally expensive and may not be affordable in preliminary design phases. To examine the importance of modeling these nonlinearities, this paper included a gallery of case studies for various support configurations with different RNA layouts, turbine loads, masses, and expected water depths. Each case was investigated with different numerical tools (SubDyn, GEBT, and ANSYS) and in linear and nonlinear modes. The cross-tool comparison

lent confidence in the results and offered initial verification of SubDyn's output.

The case studies analyzed in this paper included: a monopile, a tripod, three jacket configurations, and an all-lattice tower. Main design and load parameters are given in Table 19.

Table 19. Main Loading and Design parameters for the various cases examined in this study.

Case	*RNA mass [tonnes]*	*Assumed Thrust Levels[kN]*	*Water Depth [m]*	*Foundation Model*
Monopile/tower	350	2,000-3,500	20	Stiff (clamped base)
OC3 Tripod/tower	575	2,000-4,000	45	Stiff (clamped base)
OC4 jacket/tower	350	2,000-4,000	50	Stiff (clamped base)
7-MW turbine jacket/tower	515	2,000-4,000	40	Stiff (clamped base)
10-MW turbine jacket/tower	1,072	3,400	50	p-y curve - soil-pile interaction
All-Lattice-Tower	350	2,000-3,000	30	Stiff (clamped base)

Overall mass and modal characteristics were compared to verify accuracy with regard to the representation of the geometric models across the various tools. For simplicity, turbine loads were limited to rotor thrust vectors applied at the RNA centers of mass. Different thrust levels were analyzed to assess load-dependence effects. The magnitudes of the load vectors were varied between the maximum expected turbine thrust and an upper bound that would cause stresses above yield limits in a small portion of the support structure. Loads larger than those assumed should not occur in a reasonably designed support, thus their inclusion would artificially exaggerate the importance of nonlinearities. The deflections calculated at the tower top and the tower base (approximate location of the substructure top) were used as metrics to assess the importance of nonlinear effects.

It was observed that, in general, SubDyn agrees very well with ANSYS (run in linear mode) in both calculated modal frequencies and deflections (relative errors on the order of 0.1%). When compared to ANSYS, GEBT showed some larger discrepancies (2% to 3%) with regard to eigenfrequency results. The reason for these discrepancies was not fully investigated. Furthermore, GEBT did not provide accurate results when a transition piece was modeled as a rigid connection between the jacket and tower. In ANSYS, a rigid connection to the tower was realized via constraint equations among the interested nodes. In GEBT and SubDyn, a frame made up of high-stiffness beams was employed. GEBT showed a significant sensitivity to this aspect of the model, which was outside the scope of this study.

As expected, the RNA weight and support self-weight (overall axial compression) reduced the first natural frequencies by 2% to 3%. The magnitude of this variation decreased for higher frequency modes. In some cases, the higher eigenmodes (local member modes) exhibited an increase in frequency, likely because of the local tensile stress state that develops due to the overall structural weight action.

Compression effects associated with the RNA weight action on calculated deflections were negligible when a linear approach was used; the noted differences with cases without weight forces were due to numerical round-off errors.

In nonlinear mode, however, the RNA weight contributed to an increase in deflections of about 4% (3%-3.5%) at the tower top (base) under the thrust levels considered. This is analogous to the P-Delta effect used in civil engineering, second-order, static calculations.

In Table 20, results of this study are summarized in terms of statistics of tower-top deflection relative errors. The outputs of the various tools were compared to those obtained by ANSYS run in nonlinear mode and including the effect of the RNA weight. Although the number of analyzed cases was limited, the configurations differed vastly in geometric layouts, load intensity and paths, as well as sizes, and were thought to encompass most of the expected substructure and support designs for offshore, fixed-bottom wind applications. Therefore, the data were deemed sufficient to reach more general conclusions on the importance of nonlinearities in offshore wind substructures.

It was observed that P-Delta effects are the most important nonlinearities, and that although at tower top a 4% increase in deflection translates into a 10-cm variation, at tower base a 3.5% increase corresponds to less than 1 cm. Effectively, this means that the absolute effects of nonlinearities are mostly associated with the tower, and that the substructure is stiff enough to virtually behave linearly. Although not shown in this paper, similar conclusions can be derived by a cursory analysis of maximum stresses as calculated by ANSYS.

Additionally, variation in load magnitude showed very little effect on these results. Moving from the smaller to the larger thrust loads changed the variation in deflection between linear and nonlinear results by 2% to 5% depending on the case.

These assessments, although based on static simulations, lend confidence in the linear approach selected for SubDyn, and suggest that errors due to the ignored nonlinearities are secondary in the overall accuracy of the FAST simulation output. Furthermore, the most important nonlinear effects were observed within the tower, which is normally modeled by the FAST module ElastoDyn (not by SubDyn) where those nonlinearities are captured. Based on this study's conclusions, SubDyn was deemed an appropriate tool to be utilized within FAST to analyze multimember substructures for offshore wind applications.

Table 20. Statistics of Tower-top deflection relative difference between the results from various tools and the ANSYS nonlinear runs' results.

Code/mode	*Mean*	*Std. Deviation*	*Max*	*Min*
ANSYS linear	-3.34%	0.8%	-2.57%	-4.43%
GEBT linear	-4.28%	--	-4.28%	-4.28%
GEBT non-linear	0.05%	--	0.72%	-0.62%
SubDyn	-2.91%	0.8%	-1.97%	-4.25%

ACKNOWLEDGMENTS

This work was performed at NREL in support of the U.S. Department of Energy under contract number DE-AC36-08GO28308. The authors would like to thank Frederick Driscoll and Senu Sirnivas of NREL for their comments on this work.

REFERENCES

[1] Musial, W.D.; Butterfield, C.P. (2004). Future for Offshore Wind Energy in the United States, - *EnergyOcean Proceedings*, Palm Beach, FL, June 2004. NREL/CP-500-36313.

[2] Elliott, D., Schwartz, M., Haymes, S., Heimiller, D., Musial, W. (2011). Assessment of Offshore Wind Energy Potential in the United States (Poster). NREL. 1 pg.; NREL Report No. PO-7A20-51332.

[3] Musial, W.D.; Butterfield, S.; Ram, B. (2006). Energy from Offshore Wind.Offshore Technology Conference, Houston, TX, May 1-4, 2006. NREL/CP-500-39450.

[4] De Vries, W. et al. (2011). *Final Report WP4.2: Support Structure Concepts for Deep Water Sites*, UpWind_WP4_D4.2.8_Final Report, Project Upwind Contract No. 019945(SES6).

[5] Jonkman, J. M.; Buhl Jr., M.L. (2005). *FAST User's Guide*. NREL/EL-500-38230. National Renewable Energy Laboratory, Golden, CO.

[6] Jonkman, J.M. (2013): The New Modularization Framework for the FAST Wind Turbine CAE Tool. 51st AIAA Aerospace Sciences Meeting and 31st ASME Wind Energy Symposium, Grapevine, Texas, Jan. 2013.

[7] Song, H.; Robertson, A.; Jonkman, J.; Sewell, D. M. (2012). Incorporation of Multi-Member Substructure Capabilities in FAST for Analysis of Offshore Wind Turbines. Offshore Technology Conference, Houston, TX, April 30-May 4, 2012.

[8] Song, H; Damiani, R.; Robertson, A.; Jonkman, J. (2013). A New Structural-Dynamics Module for Offshore Multimember Substructures within the Wind Turbine CAE Tool FAST. 23rd International Ocean and Polar Engineering Conference, Anchorage, AK, June30-July 5, 2013.

[9] Yu, W.; Blair, M. (2010). A General-Purpose Implementation of the Mixed Formulation of the Geometrical Exact Beam Theory. 51st AIAA/ASME/ASCE/AHS/ASC Structures, Structural Dynamics, and Materials Conference, Orlando, FL, April 12—15, 2010.

[10] Craig, R.; Bampton, M.C.C. (1968). Coupling of substructures for dynamic analyses. *AIAA Journal*, Vol. 6, No. 7 (1968), pp. 1313-1319.

[11] Hodges, D. H. (2006). Nonlinear Composite Beam Theory. *Progress in Astronautics and Aeronautics 213*, AIAA, Reston, Virginia, 2006.

[12] Cordle, A.; McCann, G.; De Vries,W. (2011). Design Drivers for Offshore Wind Turbine Jacket Support Structures. ASME Conf. Proc. 2011, 419, DOI:10.1115/OMAE2011-49338.

[13] Jonkman, J; Musial, W. (2010). *Offshore Code Comparison Collaboration (OC3) for IEA Task 23 Offshore Wind Technology and Deployment*, Technical Report, NREL/TP-5000-48191, December 2010.

[14] Jonkman; J., Butterfield, S.; Musial W.; Scott, G. (2009). *Definition of a 5-MW Reference Wind Turbine for Offshore System Development*. National Renewable Energy Laboratory, Golden, CO. NREL/TP-5000-38060.

[15] Popko, W. et al (2012). Offshore Code Comparison Collaboration Continuation (OC4), Phase I –Results of Coupled Simulations of an Offshore Wind Turbine with Jacket Support Structure. 22nd International Society of Offshore and Polar Engineers Conference. Rhodes, Greece. June 17-22, 2012.

[16] Vorpahl, F.; Kaufer, D.; Popko, W. (2011). *Description of a Basic Model of the "Upwind Reference Jacket" for Code Comparison in the OC4 Project under IEA Wind Annex 30*. Technical report, Fraunhofer Institute for Wind Energy and Energy System Technology IWES.

[17] Damiani, R.; Song, H. (2013). A Jacket Sizing Tool for Offshore Wind Turbines within the Systems Engineering Initiative. Offshore Technology Conference, Houston, Texas, USA, 6–9 May.

[18] API (2000): RP 2A (WSD) - Recommended Practice for Planning, Designing and Constructing Fixed Offshore Platforms – Working Stress Design, 21st Edition, December, 2000, with Supplements in December, 2002, September, 2005, and October 2007.

[19] Long, H.; Moe, G.; Fischer, T. J. (2012). Lattice Towers for Bottom-Fixed Offshore Wind Turbines in the Ultimate Limit State: Variation of Some Geometric Parameters. *Journal of Offshore Mech*. Arct. Eng. **134**, 021202-1-13